Peroxone chemistry: Formation of H_2O_3 and ring-$(HO_2)(HO_3)$ from O_3/H_2O_2

Xin Xu[†] and William A. Goddard III[‡]

Materials and Process Simulation Center, Beckman Institute (MC 139-74), California Institute of Technology, Pasadena, CA 91125

Contributed by William A. Goddard III, October 2, 2002

The recent observation [Wentworth, P., Jones, L. H., Wentworth, A. D., Zhu, X. Y., Larsen, N. A., Wilson, I. A., Xu, X., Goddard, W. A., Janda, K. D., Eschenmoser, A. & Lerner, R. A. (2001) *Science* 293, 1806–1811] that antibodies form H_2O_2 from $^1O_2$ plus H_2O was explained in terms of the formation of the H_2O_3 species that in the antibody reacts with a second H_2O_3 to form H_2O_2. There have been few reports of the chemistry for forming H_2O_3, but recently Engdahl and Nelander [Engdahl, A. & Nelander, B. (2002) *Science* 295, 482–483] reported that photolysis of the ozone–hydrogen peroxide complex in argon matrices leads to significant concentrations of H_2O_3. We report here the chemical mechanism for this process, determined by using first-principles quantum mechanics. We show that in an argon matrix it is favorable (3.5 kcal/mol barrier) for H_2O_2 and O_3 to form a $[(HO_2)(HO_3)]$ hydrogen-bonded complex [head-to-tail seven-membered ring (7r)]. In this complex, the barrier for forming H_2O_3 plus $^3O_2$ is only 4.8 kcal/mol, which should be observable by means of thermal processes (not yet reported). Irradiation of the $[(HO_2)(HO_3)$-7r] complex should break the HO–OO bond of the HO_3 moiety, eliminating $^3O_2$ and leading to $[(HO_2)(HO)]$. This $[(HO_2)(HO)]$ confined in the matrix cage is expected to rearrange to also form H_2O_3 (observed experimentally). We show that these two processes can be distinguished isotopically. These results (including the predicted vibrational frequencies) suggest strategies for synthesizing H_2O_3 and characterizing its chemistry. We suggest that the $[(HO_2)(HO_3)$-7r] complex and H_2O_3 are involved in biological, atmospheric, and environmental oxidative processes.

Peroxone (the combination of ozone and hydrogen peroxide) is used to treat soil, groundwater, and wastewater contaminated with volatile organic compounds, polycyclic aromatic hydrocarbons, petroleum hydrocarbons, chlorinated solvents, metals, munitions, diesel fuel, methyl *tert*-butyl ether (MTBE), BTEX (benzene, toluene, ethylbenzene, and xylene), trinitrotoluene (TNT), and other waste constituents (1). This mixture of ozone with hydrogen peroxide is far more reactive than either alone (1), but no mechanistic studies have been reported to explain why.

A recent paper (2) showed that mixing O_3 and H_2O_2 in an argon matrix leads to a complex that when photolyzed produces significant concentrations of H_2O_3, indicating that complex intermediates might be involved in the peroxone process.

Another recent paper (3) showed the surprising result that H_2O_3 is apparently involved in the formation of H_2O_2 from $^1O_2$ plus H_2O by antibodies. Here a H_2O_3 species reacts with a second H_2O_3 to form [(HOO)(HOOO)-7r] (a head-to-tail seven-member ring complex), which subsequently leads to H_2O_2 (4, 5).

These studies suggest that other poorly understood but important oxidative processes involved in biological, atmospheric, and aqueous systems may involve H_2O_3, [(HOO)(HOOO)-7r], and related unknown or poorly characterized intermediates. Consequently we have been studying the chemistry of some of these possibly important species.

This report presents a detailed mechanistic study of the formation of H_2O_3 from $H_2O_2 + O_3$. Our results show that a complex of H_2O_2 and O_3 rearranges first to form the [(HOO)(HOOO)-7r] complex claimed in ref. 4 to be involved in the antibody-catalyzed process. Under irradiation, the HO–OO bond should break, leading to $^3O_2$ plus $[(HO_2)(HO)]$ confined in the matrix cage, which is expected to rearrange to form H_2O_3, which has been observed in ref. 2. In addition, the same cyclic intermediate complex can form H_2O_3 by a thermal unimolecular rearrangement process. We show that these two processes can be distinguished isotopically.

The computational details are given in the next section, followed by a presentation of the results, a discussion of the implications, and finally a presentation of some conclusions.

Computational Details

All quantum mechanical (QM) calculations used the B3LYP flavor of density functional theory (DFT) (6–10), which includes a generalized gradient approximation (GGA) and some exact exchange (hybrid method). The 6-31G** basis set (11, 12) was used on all atoms, and a full geometry optimization was carried out for all stable complexes and saddle points. Vibrational frequencies (from the analytic Hessian) were calculated to ensure that each minimum is a true local minimum (containing only positive frequencies) and that each transition state has only a single imaginary frequency (one negative eigenvalue of the Hessian). The Pulay modified scaled quantum mechanical (SQM) method was used to predict the vibrational frequencies (13). Scale factors for O–O stretching, O–H stretching, O–O–O bending, O–O–H bending, and O–O–O–H torsion are 0.917, 0.905, 0.920, 0.939, and 0.855, respectively. All QM calculations were carried out with JAGUAR (14).

To obtain more accurate energetics, we also carried out calculations with the cc-pVTZ basis set (15), using the optimized geometries from the 6-31G** basis. It was reported that calculations with B3LYP/6-311+G (3df,2p) lead to a mean absolute error of 3.11 kcal/mol for a collection of 148 simple inorganic/organic molecules (16).

For molecules such as $^1O_2$ and O_3, which have significant open-shell character, standard density functional theory methods often lead to much larger errors. Thus with B3LYP the singlet and triplet gap for O_2 is ΔE ($^1\Delta_g - {}^3\Sigma_g^-$) = 10.4 kcal/mol, in poor agreement with the experimental value of 22.5 kcal/mol (17). Consequently, we used spin-projection techniques (18) to ensure a proper description of the complexes involving $^1O_2$. This procedure leads to ΔE ($^1\Delta_g - {}^3\Sigma_g^-$) = 20.5 kcal/mol, in reasonable agreement with experiment.

Fig. 1 summarizes the whole reaction profile from $H_2O_2 + O_3$ to $H_2O_3 + O_2$, where LM stands for "local minimum" and TS stands for "transition state." All energetics are reported for ΔH (298 K), in kcal/mol, where the calculated vibrational frequencies were used with standard quantum statistical formulas to obtain the entropy and enthalpy as a function of temperature.

Abbreviation: LM, local minimum.

[†]On sabbatical leave from Xiamen University, Xiamen 361005, China.

[‡]To whom correspondence should be addressed. E-mail: wag@wag.caltech.edu.

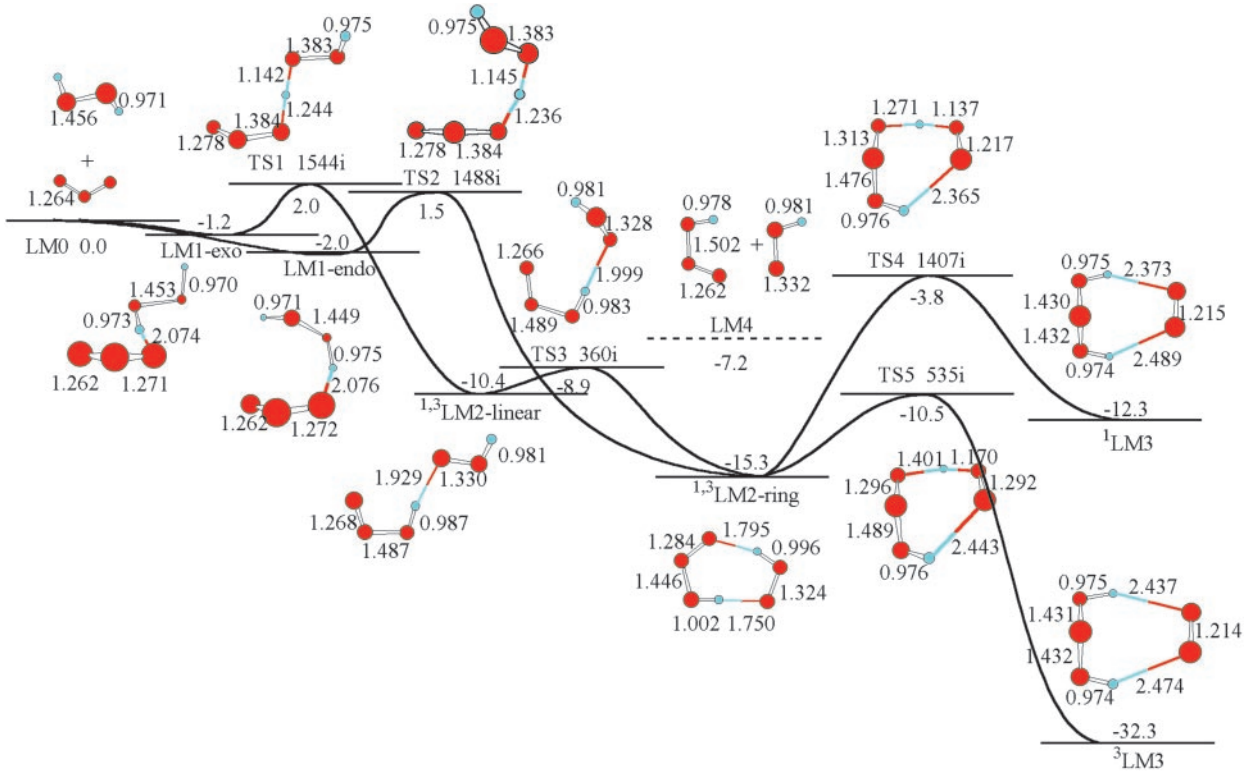

Fig. 1. Reaction profile from $H_2O_2 + O_3$ to $H_2O_3 + {}^3O_2$. TS, transition state.

Results

Formation of [$(HO_2)(HO_3)$-7r] Cyclic Complex. Starting with the free reactants (LM0: $H_2O_2 + O_3$), we find two molecular complexes, LM1-endo and LM1-exo: $[(H_2O_2)(O_3)]$, leading to Eqs. **1a** and **1b**.

$$\underset{0.0}{\text{LM0: } H_2O_2 + O_3} \rightarrow \underset{-1.2}{\text{LM1-exo: } [(H_2O_2)(O_3)]} \qquad \textbf{[1a]}$$

$$\underset{0.0}{\text{LM0: } H_2O_2 + O_3} \rightarrow \underset{-2.0}{\text{LM1-endo: } [(H_2O_2)(O_3)]} \qquad \textbf{[1b]}$$

where LM1-endo has a pseudoring configuration and LM1-exo has a pseudolinear configuration (see Fig. 1). LM1 can be formally considered as $\sigma-$complexes with H of H_2O_2 pointing to the P_σ lone pair orbital of a terminal O of O_3. This hydrogen bond is weak (2.0 kcal/mol, compared with 5.0 kcal/mol for water dimer) because the Mulliken charge on the terminal oxygen is only -0.2 (compared with -0.6 in H_2O).

We find LM1-exo leads to the formation of LM2-linear: $[(HO_2)(HO_3)$-L], whereas LM1-endo leads to the formation of LM2-ring: $[(HO_2)(HO_3)$-7r] (seven-member ring), as in Eqs. **2a** and **2b**. In addition, LM2-linear can rearrange to LM2-ring as in Eq. **2c**.

$$\underset{0.0}{\text{LM1-exo: } [(H_2O_2)(O_3)]} \rightarrow \underset{3.5}{\text{TS1}} \rightarrow \underset{-8.4}{\text{LM2-linear: } [(HO_2)(HO_3)\text{-L}]} \qquad \textbf{[2a]}$$

$$\underset{0.0}{\text{LM1-endo: } [(H_2O_2)(O_3)]} \rightarrow \underset{3.2}{\text{TS2}} \rightarrow \underset{-14.1}{\text{LM2-ring: } [(HO_2)(HO_3)\text{-7r}]} \qquad \textbf{[2b]}$$

$$\underset{0.0}{\text{LM2-linear: } [(HO_2)(HO_3)\text{-L}]} \rightarrow \underset{1.5}{\text{TS3}} \rightarrow \underset{-4.9}{\text{LM2-ring: } [(HO_2)(HO_3)\text{-7r}]} \qquad \textbf{[2c]}$$

The barrier is 3.5 kcal/mol from LM1-exo to LM2-linear, whereas it is 3.2 kcal/mol from LM1-endo to LM2-ring. Both reactions are noteworthy in that they convert the closed-shell singlet molecules H_2O_2 and O_3 to a biradical complex $[(HO_2)(HO_3)]$, which is significantly more stable (10.4 kcal/mol for linear and 15.3 for cyclic) than the free reactants $H_2O_2 + O_3$. Both products LM2-linear and LM2-ring are planar, with the radical (singly occupied) orbitals perpendicular to the molecular plane. In the HOO moiety, ≈70% of the spin density is localized at the terminal oxygen, whereas in the HOOO moiety, ≈90% of the spin density is on the two terminal oxygens. In this biradical the energy surface for the spin singlet initial state is degenerate with the triplet surface (we calculate that the singlet state is 0.01 kcal/mol lower), leading to rapid interconversion to the triplet. (The rate is determined by the spin orbit matrix elements and the energy spacings between the various populated vibrational—rotational levels, which we guess might be microseconds.) Neglecting decomposition and reactions from this state, the equilibrium concentration ratio of triplet to singlet would be 3:1.

It was reported that codepositing O_3 and H_2O_2 in argon matrices leads to new IR bands indicating complex formation, but no details were reported (2). We predict that this complex is most likely to be the cyclic $[(HO_2)(HO_3)$-7r] complex (LM2-ring). To help test this prediction, we report the predicted vibrational frequencies in Table 1 for various isotopic cases.

Formation of H_2O_3 by Thermal Processes. Starting with the LM2-ring complex, a simple H atom transfer process allows the hydrogen of HO_2 to transfer to the terminal oxygen of HO_3, leading

CHEMISTRY

Table 1. Predicted fundamentals for the [$(HO_2)(HO_3)$-7r] complex, in wavenumbers, based on the scaled quantum mechanical analysis of the Hessian from B3LYP/6-31G calculations**

Mode	Character	Wavenumber, cm^{-1}		
		$(HO_2)(HO_3)$	$(HO_2)(H^{18}O_3)$	$(DO_2)(DO_3)$
ν_1	Antisymmetric OH stretch	3,190.3 (737.3)	3,188.8	2,331.8
ν_2	Symmetric OH stretch	3,030.1 (260.9)	3,020.6	2,220.2
ν_3	HOO bend of HO_3	1,511.6 (64.7)	1,506.1	1,216.9
ν_4	HOO bend of HO_2	1,466.9 (65.4)	1,460.1	1,180.5
ν_5	OO stretch of HO_2	1,173.8 (9.1)	1,173.7	1,096.3
ν_6	Symmetric OO stretch of HO_3	1,167.2 (29.7)	1,102.7	1,074.7
ν_7	Antisymmetric OO stretch of HO_3	956.8 (72.1)	956.3	780.5
ν_8	HOOO-oop	787.9 (100.6)	743.6	690.8
ν_9	HO_2–HO_3-slide	588.5 (161.4)	588.1	512.0
ν_{10}	O–O–O bend in HO_3	533.2 (5.6)	505.0	432.3
ν_{11}	Antisymmetric hydrogen-bond stretch	273.2 (49.9)	271.4	261.8
ν_{12}	Ring torsion-twist	219.6 (3.2)	210.2	216.8
ν_{13}	Symmetric hydrogen-bond stretch	175.1 (1.9)	171.1	170.4
ν_{14}	Ring torsion-chair	116.3 (0.5)	110.3	116.0
ν_{15}	Ring torsion-boat	65.3 (0.8)	64.7	64.2

The calculated infrared intensities for [$(HO_2)(HO_3)$-7r] are listed in parentheses.

directly to the formation of HOOOH, as indicated in Eq. **3** (see Fig. 1). Because the LM2-ring is expected to have nearly degenerate singlet and triplet spin states, we considered both spin states.

$$\underset{0.0}{{}^1\text{LM2-ring: } {}^1[(HO_2)(HO_3)\text{-7r}]} \rightarrow \underset{11.5}{\text{TS4: } [O_2 \cdots H \cdots O_3H]} \rightarrow \underset{3.0}{{}^1\text{LM3: } [({}^1O_2)(H_2O_3\text{-c})]} \quad \textbf{[3a]}$$

$$\underset{0.0}{{}^3\text{LM2-ring: } {}^3[(HO_2)(HO_3)\text{-7r}]} \rightarrow \underset{4.8}{\text{TS5: } [O_2 \cdots H \cdots O_3H]} \rightarrow \underset{-17.0}{{}^3\text{LM3: } [({}^3O_2)(H_2O_3\text{-c})]} \quad \textbf{[3b]}$$

For the triplet case, the net reaction is 17.0 kcal/mol exothermic (because of formation of the ground state triplet molecule, $^3O_2$), leading to a barrier of only 4.8 kcal/mol. Forming $^1O_2$ is endothermic by 3.0 kcal/mol with a barrier of 11.5 kcal/mol. Thus at low temperatures the triplet process is expected to dominate. Because of the rapid singlet–triplet conversion in $[(HO_2)(HO_3)$-7r], it is likely to produce H_2O_3 even at low temperature.

The H_2O_3 formed in Eqs. **3a** and **3b** is in the *cis* form, with both O–H groups pointing toward the same side of the O–O–O plane of H_2O_3 (See Fig. 1). The O_2 and H_2O_3 complexes (LM3) formed are very weakly bound (binding energy = 0.2 kcal/mol), so that they are likely to dissociate even in the matrix.

The *cis* H_2O_3 can rotate its OH bond (either inward or outward) to convert to the *trans* global minimum of H_2O_3 with a low barrier as in Eq. **4** (refs. 4 and 19; ref. 19 reported detailed theoretical studies of H_2O_3).

Starting with $^{18}O_3 + H_2O_2$, the thermal process would lead to the formation of $H^{18}O^{18}O^{18}OH$. Table 2 gives the predicted vibrational frequencies, which should be useful for experimental validation of these results.

$$\underset{0.0}{H_2O_3\text{-c}} \rightarrow \underset{2.9/3.3}{\text{TS6 (outward)/TS7 (inward)}} \rightarrow \underset{-2.4}{H_2O_3\text{-t}} \quad \textbf{[4]}$$

Formation of H_2O_3 by Photolysis. We find that free HOOO radical has a planar *cis* configuration. It is bound by only 3 kcal/mol with respect to HO and $^3O_2$, with a barrier to decomposition of only 4 kcal/mol.

Table 2. Predicted fundamentals of *cis* HOOOH and *trans* HOOOH, $H^{18}OOOH$, $H^{18}O^{18}O^{18}OH$, HOOOD, and DOOOD, in wavenumbers, based on the scaled quantum mechanical analysis of the Hessian from B3LYP/6-31G calculations**

Molecule	Wavenumber, cm^{-1}								
	ν_1	ν_2	ν_3	ν_4	ν_5	ν_6	ν_7	ν_8	ν_9
H_2O_3-c	3,522.0	3,518.7	1,359.9	1,329.5	900.7	768.0	485.5	418.4	190.4
H_2O_3-t	3,533.1	3,528.4	1,353.6	1,349.6	899.5	770.2	506.5	410.4	346.9
	(3,529.6)	(3,529.6)	(1,359.1)	(1,347.4)	(821.0)	(776.3)	(509.1)	(387.0)	(346.4)
$H^{18}OOOH$-t	3,531.2	3,518.3	1,352.4	1,347.0	887.6	759.9	495.1	408.9	346.3
	(3,529.6)	(3,520.3)	(1,357.0)	(1,344.3)	(NR)	(768.0)	(NR)	(386.6)	(346.0)
$HO^{18}OOH$-t	3,528.4	3,533.1	1,348.7	1,347.0	874.8	745.6	502.9	408.4	346.1
$H_2{}^{18}O_3$-t	3,521.1	3,516.4	1,344.8	1,343.8	848.3	726.1	480.3	405.6	344.8
HO_3D-t	3,530.7	2,580.5	1,351.4	1,009.2	896.3	770.0	499.5	387.1	276.6
	(3,529.6)	(2,610.4)	(1,349.9)	(NR)	(814.6)	(772.0)	(NR)	(369.2)	(NR)
D_2O_3-t	2,582.2	2,579.0	1,013.6	1,004.2	892.8	769.8	492.6	317.1	252.8
	(2,610.4)	(2,610.4)	(1,007.3)	(NR)	(NR)	(762.6)	(NR)	(301.6)	(273.5)

The experimental data (2) are listed in parentheses for comparison (NR, not reported). The modes are as follows: ν_1, symmetric OH stretch; ν_2, antisymmetric OH stretch; ν_3, antisymmetric HOO bend; ν_4, symmetric HOOO bend; ν_5, symmetric OO stretch; ν_6, antisymmetric OO stretch; ν_7, OOO bend; ν_8, antisymmetric torsion; and ν_9, symmetric torsion.

$$\underset{0.0}{\text{HOOO-cis}} \rightarrow \underset{3.7}{\text{TS8: HO}\cdots\text{OO}} \rightarrow \underset{2.8}{\text{HO} + {}^3\text{O}_2} \qquad \textbf{[5]}$$

This configuration is consistent with the experimental observation that HOOO can be formed when hydroxyl radicals are added to molecular oxygen in an argon matrix (20). The terminal OO bond in HOOO is 1.26 Å, indicating a partial double bond resulting from π resonance (just as in HOO), whereas the other OO bond is 1.50 Å, slightly longer than a single bond (1.46 Å) in H_2O_2. Thus photolyzing HOOO is expected to break the weak bond between HO and OO, producing HO + $^3O_2$ by a spin-allowed process.

[$(HO_2)(HO_3)$-7r] is stabilized by 8.1 kcal/mol (Eq. **6**), which should retard the decomposition of HO_3.

$$\text{LM2-ring: } {}^3[(HO_2)(HO_3)\text{-7r}] \underset{0.0}{\rightarrow} \underset{8.1}{HO_2 + HO_3} \rightarrow \underset{10.9}{HO_2 + HO + {}^3O_2} \qquad \textbf{[6]}$$

Because the barrier for the thermal process to produce H_2O_3 + $^3O_2$ is only 4.8 kcal/mol, we expect that reaction **6** would not be so important in a low-temperature process.

Photolysis of [$(HO_2)(HO_3)$-7r] is expected to produce $^3O_2$, leaving behind a [(HOO)(HO)] complex in the matrix cage. Because [$(HO_2)(HO_3)$-7r] is ≈75% triplet, we expect the [(HOO)(HO)] complex formed in this decomposition to be predominantly singlet as in Eq. **7**, which can close rapidly to form HOOOH as in Eq. **8**

$$[(\text{HOO}^{\uparrow})(\text{HO}^{\downarrow}\,{}^{\uparrow}\text{OO}^{\uparrow})\text{-7r}] \rightarrow \text{HOO}^{\uparrow}\cdots\text{HO}^{\downarrow} + {}^3\text{O}_2 \qquad \textbf{[7]}$$

$$\text{HOO}^{\uparrow}\cdots\text{HO}^{\downarrow} \rightarrow \text{HOOOH-t} \qquad \textbf{[8]}$$

Assuming no bonding in the $HOO^{\uparrow}\cdots HO^{\downarrow}$ on the left of Eq. **8**, reaction **8** is 28.2 kcal/mol exothermic. In this case the product is expected to be dominantly in the *trans* form.

In contrast, reacting gas phase HO with HOO (in an overall triplet state) leads to H_2O + $^3O_2$ with no effective barrier (21§).

$$\underset{0.0}{\text{HO} + \text{HOO}} \rightarrow \text{HO}\cdots\text{HOO} \rightarrow \underset{-66.2}{\text{H}_2\text{O} + {}^3\text{O}_2} \qquad \textbf{[9]}$$

Thus the gas-phase reaction of HO with HOO would lead mostly to water with very little formation of HOOOH.

Experimentally, photolysis at 266 nm converts the initial complex [which we predict to be ring-$(HO_2)(HO_3)$] completely to water plus a species identified as H_2O_3 by the presence of two torsion bands and two OO stretches (2). Starting with $^{18}O_3$ and H_2O_2, the photolysis experiment leads to formation of 100% $H^{18}OOOH$ (2). This result is consistent with our mechanism (from Eqs. **1** and **2** to **7** and **8**), which also leads exclusively to the formation of $H^{18}OOOH$. Table 2 summarizes the calculated frequencies of various isotopes of HOOOH, which are in good agreement with experiment (2).

Ref. 2 presented an alternative mechanism for the authors' observation of 100% $H^{18}OOOH$. They speculated that in their experiments irradiation at 266 nm decomposed O_3 to $O(^1D)$ and $O_2(^1\Delta)$ and that $O(^1D)$ inserted into the O–H of HOOH to make $H^{18}OOOH$. However, we believe that $O(^1D)$ might also insert into the OO bond of HOOH, leading to $HO^{18}OOH$. Thus we believe that this mechanism would give a mixture of $H^{18}OOOH$ and $HO^{18}OOH$, in disagreement with their experiments.

Decomposition of H_2O_3. Experimentally, prolonged irradiation eventually eliminates the bands assigned to HOOOH (2). Indeed, we find

$$\underset{0.0}{\text{HOOOH-t}} \rightarrow \underset{28.2}{\text{HO} + \text{HO}_2} \qquad \textbf{[10]}$$

The HO and HO_2 formed here can go through reaction **9**, leading to the formation of H_2O + $^3O_2$.

We also find that H_2O can catalyze the decomposition of HOOOH to $^1O_2$ (4, 22). Thus

$$\underset{0.0}{\text{H}_2\text{O}_3\text{-t}} \rightarrow \underset{44.9}{\text{TS9}} \rightarrow \underset{-16.2}{{}^1\text{O}_2 + \text{H}_2\text{O}} \qquad \textbf{[11a]}$$

$$\underset{0.0}{\text{H}_2\text{O}_3\text{-t} + \text{H}_2\text{O}} \rightarrow \underset{-7.3}{[(\text{H}_2\text{O}_3)(\text{H}_2\text{O})]} \rightarrow \underset{12.7}{\text{TS10}} \rightarrow \underset{-16.2}{{}^1\text{O}_2 + 2\text{H}_2\text{O}} \qquad \textbf{[11b]}$$

$$\underset{0.0}{\text{H}_2\text{O}_3\text{-t} + 2\text{H}_2\text{O}} \rightarrow \underset{-17.5}{[(\text{H}_2\text{O}_3)(\text{H}_2\text{O})_2]} \rightarrow \underset{0.2}{\text{TS11}} \rightarrow \underset{-16.2}{{}^1\text{O}_2 + 3\text{H}_2\text{O}} \qquad \textbf{[11c]}$$

Thus complexes of one or two H_2O with H_2O_3-t lead to decomposition barriers of 20.0 and 17.7 kcal/mol.

Discussion

Hydrogen peroxide, H_2O_2, is a widely known oxidant, but little is known of the stability and chemistry of higher hydrogen polyoxides. H_2O_3 has been postulated repeatedly (since Bertholet in 1880) to rationalize processes in combustion, explosions, atmospheric chemistry, water chemistry, biochemistry, and the radiation chemistry in aqueous systems (3–5, 22–32), but until recently it has not been known how or whether H_2O_3 is formed, when H_2O_3 can exist, and under which circumstances H_2O_3 will decompose. Thus H_2O_3 was proposed as a transient intermediate in the oxygenation of alkanes with ozone in superacid media (30) and in the pulse radiolysis of air-saturated perchloric acid solution (23). By means of ^{17}O NMR spectroscopy, Plesnicar and coworkers (32) concluded that the low-temperature ozonation of isopropyl alcohol and isopropyl methyl ether yields hydrogen trioxide H_2O_3 (in addition to the hydrotrioxides of these compounds). Recently the antibody-catalyzed oxidation of water to hydrogen peroxide by $^1O_2$ has been proposed to proceed through H_2O_3 as the critical intermediate (3–5).

This situation has changed with the recent synthesis of H_2O_3 in argon matrices by the photolysis of the ozone–hydrogen peroxide complex (2), and we have now clarified the mechanism by using first-principles quantum mechanics. We find that H_2O_3 is formed from the [$(HO_2)(HO_3)$-7r] precursor by both thermal and photolytic processes. Interestingly, use of labeled ozone ($^{18}O_3$) is predicted to yield $H^{18}O^{18}OH$ by the thermal process and $H^{18}OOOH$ by the photochemical process. We report the predicted vibrational frequencies to aid in experimentally characterizing [$(HO_2)(HO_3)$-7r] and its chemistry and for developing strategies for synthesizing it and H_2O_3.

Our calculations reveal that formation of H_2O_3 from H_2O_2 + O_3 is favorable both thermodynamically and kinetically. Irradiation of H_2O_3 with 266-nm radiation produces radicals (HO, HO_2) that can form water, which would in turn induces H_2O_3 decomposition by reactions **10** and **11b** and **11c**. Thus we anticipate that systems in which the H_2O_3 is formed by thermal processes should exhibit a much longer lifetime for the H_2O_3

§As pointed out in ref. 21, we find that the planar $^3A''$ HO···HO_2 has one imaginary frequency for the H–O···H bending, thus is not a true local minimum. Nonplanar HO···HO_2 structure leads automatically to H_2O + $^3O_2$.

than those in which the H_2O_3 is formed photolytically (because this would also form H_2O).

We suggest that [$(HO_2)(HO_3)$-7r] and H_2O_3 may both play roles in oxidative processes ranging from the peroxone environmental cleanup process to the antibody conversion of $^1O_2$ and H_2O to H_2O_2. Free OH is often postulated to be the reactive intermediate in such systems, despite the short lifetime. [$(HO_2)(HO_3)$-7r] is essentially a capped OH radical, giving it a much longer lifetime than free OH. Thus the chemistry of [$(HO_2)(HO_3)$-7r] would resemble that of free OH. For example, attack on an aromatic ring might proceed as

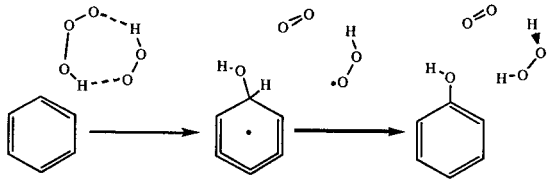

where the HO_2 in the complex can extract the H from the ring after attack by the OH.

It has long been recognized that hydrogen peroxide is an efficient catalyst for the decomposition of ozone (33) but that peroxone ($O_3 + H_2O_2$) is effective at destroying organic contaminants in water chemistry (1). We believe that the spectacular effectiveness of the peroxone process results from a variety of reactive intermediates (H_2O_3, [$(HO_2)(HO_3)$-7r]) and their products (HO_3, HO_2, OH). Knowledge of the mechanistic details connecting these species should help to understand and improve the peroxone processes for environmental applications and should help establish the role of these intermediates in a variety of biological and environmental oxidations.

These same reactive intermediates (H_2O_3, [$(HO_2)(HO_3)$-7r]) and their products (HO_3, HO_2, OH) might also be formed in the atmosphere, where conditions of low temperature and low H_2O concentrations might lead to modest concentrations of such intermediates. It is hoped that the mechanistic analysts and vibrational frequencies for the various intermediates provided here might help identify these species in atmospheric or laboratory experiments.

Conclusions

Detailed mechanisms for the formation of H_2O_3 from $H_2O_2 + O_3$ are explored in this report. We predict that the codepositing of O_3 and H_2O_2 in an argon matrix leads to formation of the [$(HO_2)(HO_3)$-7r] head-to-tail cyclic complex. We have predicted the vibrational frequencies of this complex to aid experimental validation.

We predict that thermal decomposition of [$(HO_2)(HO_3)$-7r] (by means of hydrogen transfer from the HO_2 moiety to the HO_3 moiety) will lead directly to H_2O_3 (with all 3 O atoms arising from the O_3), whereas H_2O will decompose this species to form $^1O_2$ plus H_2O. These predictions should help to define optimal experimental conditions for making H_2O_3.

On the other hand, UV irradiation of the [$(HO_2)(HO_3)$-7r] complex will break the HO–OO bond of the HO_3 moiety, eliminating $^3O_2$ and forming a [$(HO_2)(HO)$] complex. We expect that this [$(HO_2)(HO)$] confined in the matrix cage will rearrange to form H_2O_3. In this case just one of the terminal O atoms comes from O_3. This formation of only $H^{18}OOOH$ from $^{18}O_3$ has been observed experimentally.

We suggest that [$(HO_2)(HO_3)$-7r] and H_2O_3 are involved in biological, atmospheric, and environmental oxidative processes.

We thank Prof. Richard Lerner for pointing out the peroxone process and some references to us. This research was funded by National Institutes of Health Grant HD 36385-02 and the National Science Foundation. The facilities of the Materials and Process Simulation Center used in these studies were funded by a Shared University Research Grant from IBM and grants from the Defense University Research Instrumentation Program (Army Research Office and Office of Naval Research) and the National Science Foundation Major Research Instrumentation. In addition, the Materials and Process Simulation Center is funded by grants from the Department of Energy–Accelerated Strategic Computing Initiative–Academic Strategic Alliances Program, Army Research Office Multidisciplinary University Research Initiative, National Institutes of Health, National Science Foundation, ChevronTexaco, Seiko-Epson, Kellogg's, 3M, Asahi Kasei, Nippon Steel, and Toray.

1. Prousek, J. (1996) *Chem. Listy* **90,** 229–237.
2. Engdahl, A. & Nelander, B. (2002) *Science* **295,** 482–483.
3. Wentworth, P., Jones, L. H., Wentworth, A. D., Zhu, X. Y., Larsen, N. A., Wilson, I. A., Xu, X., Goddard, W. A., Janda, K. D., Eschenmoser, A. & Lerner, R. A. (2001) *Science* **293,** 1806–1811.
4. Xu, X., Muller, R. P. & Goddard, W. A., III. (2002) *Proc. Natl. Acad. Sci. USA* **99,** 3376–3381.
5. Datta, D., Vaidehi, N., Xu, X. & Goddard, W. A., III (2002) *Proc. Natl. Acad. Sci. USA* **99,** 2636–2641.
6. Slater, J. C. (1951) *Phys. Rev.* **81,** 385.
7. Vosko, S. H., Wilk, L. & Nusair, M. (1988) *Can. J. Phys.* **58**, 1200–1211.
8. Becke, A. D. (1980) *Phys. Rev. A* **38,** 3098–3100.
9. Becke, A. D. (1993) *J. Chem. Phys.* **98,** 5648–5652.
10. Lee, C. T., Yang, W. T. & Parr, R. G. (1988) *Phys. Rev. B* **37**, 785–789.
11. Hehre, W. J., Ditchfield, R. & Pople, J. A. (1972) *J. Chem. Phys.* **56,** 2257–2261.
12. Hariharan, P. C. & Pople, J. A. (1973) *Theor. Chim. Acta* **28,** 213–222.
13. Baker, J., Jarzecki, A. A. & Pulay, P. (1998) *J. Phys. Chem. A* **102,** 1412–1424.
14. Schrödinger, Inc. (1998) JAGUAR (Schrödinger, Portland, OR), Version 3.5.
15. Dunning, T. H., Jr. (1989) *J. Chem. Phys.* **90,** 1007–1023.
16. Curtiss, L. A., Raghavachari, K., Redfern, P. C. & Pople, J. A. (1997) *J. Chem. Phys.* **106,** 1063–1079.
17. Herzberg, G. (1965) *Spectra of Diatomic Molecules, Molecular Spectra, and Molecular Structure* (Van Nostrand, New York), Vol. 1, p. 560.
18. Wittbrodt, J. M. & Schlegel, H. B. (1996) *J. Chem. Phys.* **105,** 6574–6577.
19. Cremer, D. (1978) *J. Chem. Phys.* **69**, 4456–4471.
20. Nelander, B., Engdahl, A. & Svensson, T. (2000) *Chem. Phys. Lett.* **332,** 403–408.
21. Gonzalez, C., Theisen, J., Schlegel, H. B., Hase, W. L. & Kaiser, E. W. (1992) *J. Phys. Chem.* **96**, 1767–1774.
22. Koller, J. & Plesnicar, B. (1996) *J. Am. Chem. Soc.* **118,** 2470–2472.
23. Czapski, G. & Bielski, B. H. J. (1963) *J. Phys. Chem.* **67,** 2180–2184.
24. Giguere, P. A. & Herman, K. (1970) *Can. J. Chem.* **48,** 3473–3482.
25. Nangia, P. S. & Benson, S. W. (1979) *J. Phys. Chem.* **83,** 1138–1142.
26. Diem, M., Tso, T.-L. & Lee, E. K. C. (1982) *J. Chem. Phys.* **76,** 6452–6454.
27. Sugimoto, H. & Sawyer, D. T. (1988) *J. Am. Chem. Soc.* **110,** 8707–8708.
28. Plesnicar, B., Kovac, F. & Schara, M. (1988) *J. Am. Chem. Soc.* **110,** 214–222.
29. Plesnicar, B., Cerkovnik, J., Koller, J. & Kovac, F. (1991) *J. Am. Chem. Soc.* **113,** 4946–4953.
30. Cerkovnik, J. & Plesnicar, B. (1993) *J. Am. Chem. Soc.* **115,** 12169–12170.
31. Speranza, M. (1996) *Inorg. Chem.* **35,** 6140–6151.
32. Plesnicar, B., Cerkovnik, J., Tekavec, T. & Koller, J. (2000) *Chem. Eur. J.* **6,** 809–819.
33. Bray, W. C. (1938) *J. Am. Chem. Soc.* **60,** 82–87.